Rationalization of the formation and stability of bosutinib solvated forms

Eszter Tieger*[1,2], Violetta Kiss[2§,3], György Pokol[1], Zoltán Finta[4], Jan Rohlíček[5], Eliška Skořepová[2,6], Michal Dušek[5]

[1]Department of Inorganic and Analytical Chemistry, Budapest University of Technology and Economics, Szt. Gellért tér 4, 1111 Budapest, Hungary, tiegereszter@gmail.com

[2] Zentiva k.s., U kabelovny 130, 102 37, Prague, Czech Republic

[3]Janssen Pharmaceuticals, Inc. - Pharmaceutical Companies of Johnson & Johnson, Turnhoutseweg 30, B-2340 Beerse, Belgium

[4]Chinoin Zrt., Tó utca 1-5., 1045 Budapest, Hungary

[5] Institute of Physics of the Czech Academy of Sciences, Na Slovance 2, 182 21 Prague, Czech Republic

[6]Department of Solid State Chemistry, University of Chemistry and Technology, Prague, Technicka 5, 166 28 Prague, Czech Republic

Preparation of the phases

**Table S1** Applied crystallization media

Phase	Crystallization media
7H_2O	Acetone:water 1:2:
6H_2O	Acetonitrile:water 92:8
IPA-2H_2O	2-propanol:water 2:1
MeOH(H_2O)	Methanol
Diox-2H_2O	1,4-Dioxane:water 1:1
DMSO-3H_2O	Dimethyl sulfoxide:water 3:1
2-BuOH	2-Butanol

---

§ Formerly Zentiva k.s., currently Janssen Pharmaceuticals, Inc.

Refinement of the structure of AH

The result list of the structure solution process contained several results with lowest values of the cost-function and showing the identical positions of the quinoline and phenyl part of the bosutinib molecule but significantly different positions of the 4-methylpiperazin ring, as it is depicted in Figure S1. Rietveld refinement of the best result from the list has shown several positive and negative peaks ($\Delta\rho$: -0.52 and 0.56 eÅ^{-3}) in the difference Fourier map either at atomic positions or very close to the 4-methylpiperazin ring. For these two reasons, we decided to introduce a disorder. After introducing the disorder containing 4-methylpiperazin ring and propionyl chain (according to the two most common different positions in the result list), agreement factors decreased from R_{wp} = 5.98 to R_{wp} = 4.98 ($\Delta\rho$: -0.45 and 0.44 eÅ^{-3}). One would expect that the change of the R-values would be more significant. This is probably caused by the non-optimal description of the disorder. We have tested another description of the disorder, but it resulted with higher R-values.
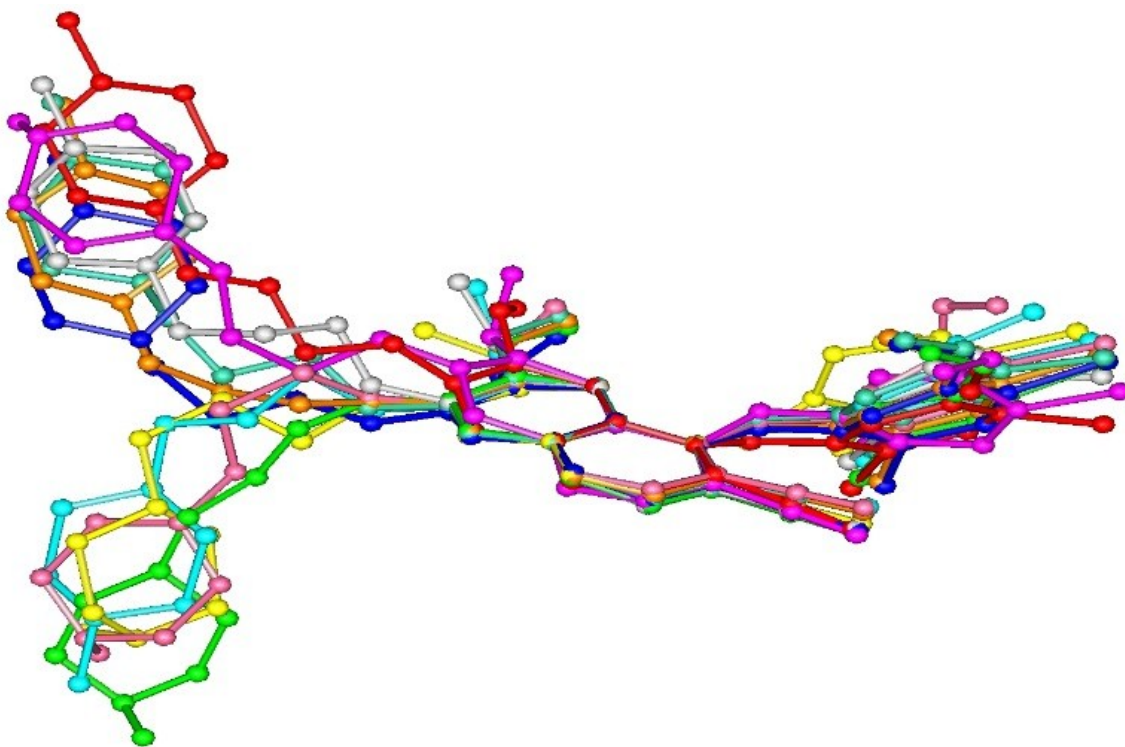
Figure S1 Overlapped 10 molecules of bosutinib as suggested by FOX program during the structure solution process. Overlapped results with comparable cost-functions has identical packing, the only significant difference is the position of methylpiperazin ring

Refinement of the structure of 1H₂O-II

In the case of $1H_2O$-II, even if the quality of the measured powder diffraction data was very low, it was possible to locate the water molecule in one of the void space. Removing the water molecule from the refinement, performing several cycles of the refinement, and calculation of the difference Fourier map revealed an elongated maximum in the previous position of the water molecule, see Figure S2. The crystal structure contains a void space with the centre at (0.5, 0, 0) without any reasonable maximum in the difference Fourier map indicating the presence of the water molecule. Despite of that, we decided to test the presence of water molecule in this void space by adding one oxygen atom in the middle. After refining, the calculation of the difference Fourier map shows significant minimum at the position of this second water molecule. Together with increasing R-factors (from $R_{wp} = 2.91$ to $R_{wp} = 3.32$) it indicates, that this void space is most probably empty.

contour level: 0.3 e/Å³   2.73 Å

2.45 Å
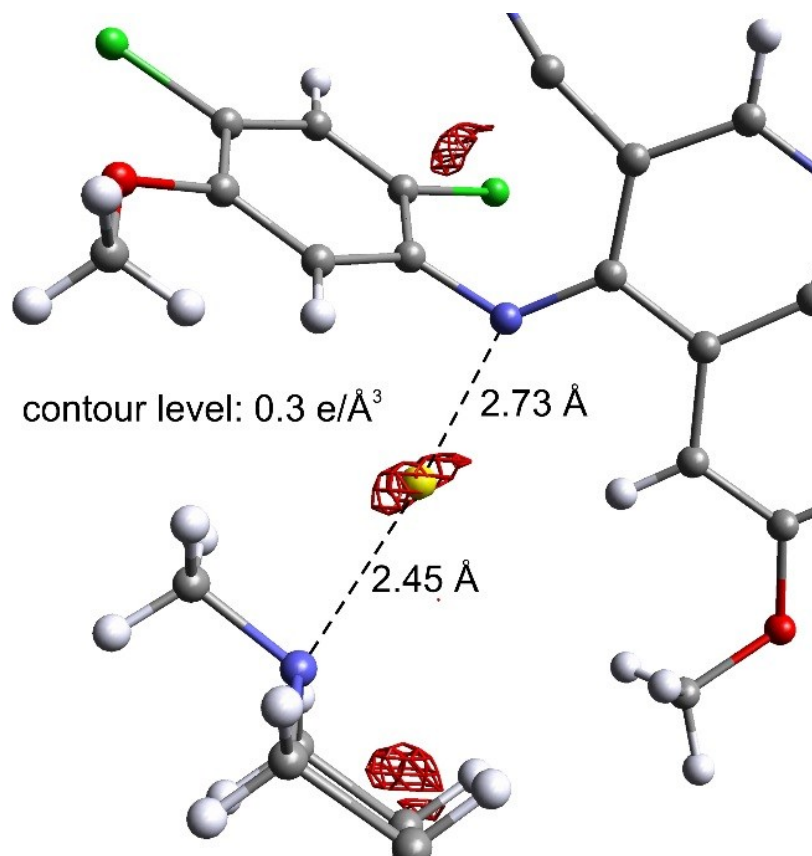
Figure S2 Maximum of the difference Fourier map shown in the program MCE[**]. The red contour map shows the positive level at 0.3 eÅ⁻³. The yellow "atom" indicates maximum of the difference Fourier map, which is in a good agreement with the position of the water molecule

---

[**] J. Rohlícek, M. Husák, MCE2005 - a new version of a program for fast interactive visualization of electron and similar density maps optimized for small molecules, J. Appl. Cryst. 2007, 40, 600-601

The refinement of the structure of AH was originally performed at 150K and $1H_2O$-II at 298 K, but the structures were measured at 120K as well in order to compare their density and packing efficiency to the other structures. The original crystal data is summarized in Table S2.

Table S2 Original crystal data of AH and 1H2O-II

	AH	**1H$_2$O–II**
Formula	$C_{26}H_{29}Cl_2N_5O_3$	$C_{26}H_{31}Cl_2N_5O_4$
Cell parameters	a=24.187 (11) b=8.112 (2) c=13.022 (6) α=90 β=91.868 (3) γ=90	a=9.588 (6) b=12.476 (12) c=12.972 (7) α=80.606 (4) β=77.792 (4) γ=71.174 (4)
Volume	2553.55 Å^3	1427.84 Å^3
Crystal system	Monoclinic	Triclinic
Space group	$P\,2_1/a$	$P\,$-1
R-factor	0.0766	0.0766
Density	1.38 g/cm^3	1.269 g/cm^3
Temperature	150 K	298 K
Z	4	2

Molecular configuration
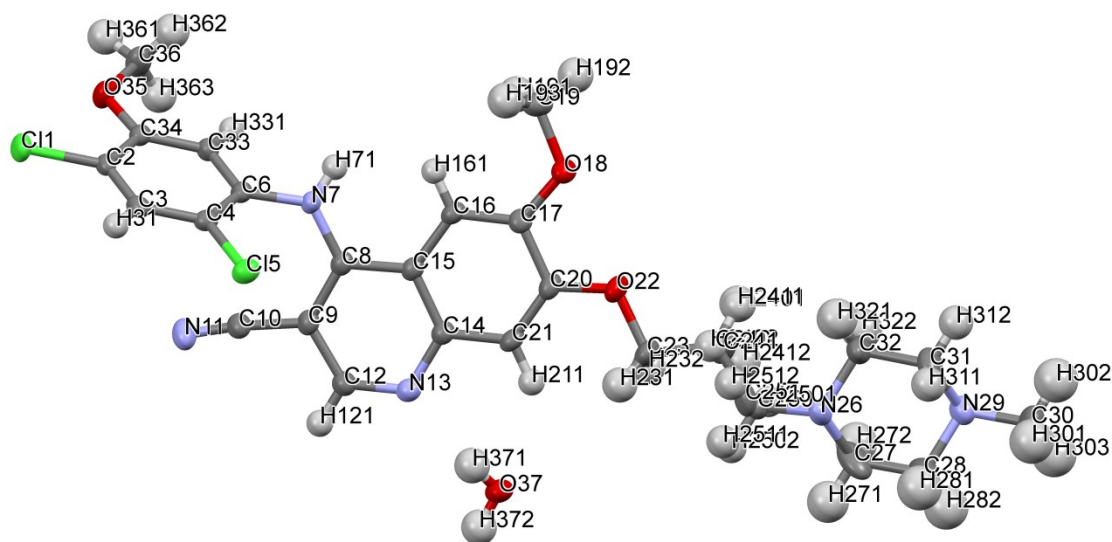
Figure S3 Molecular configuration and atom-numbering scheme for 1H$_2$O-I
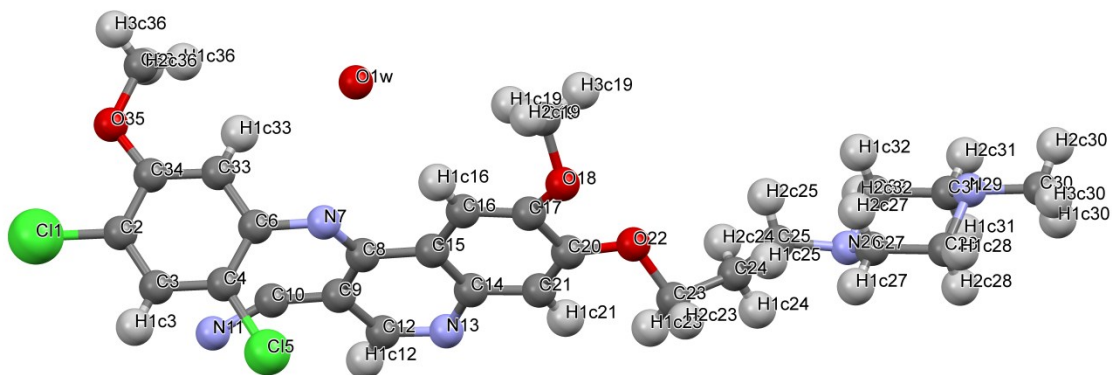
Figure S4 Molecular configuration and atom-numbering scheme for 1H$_2$O-II

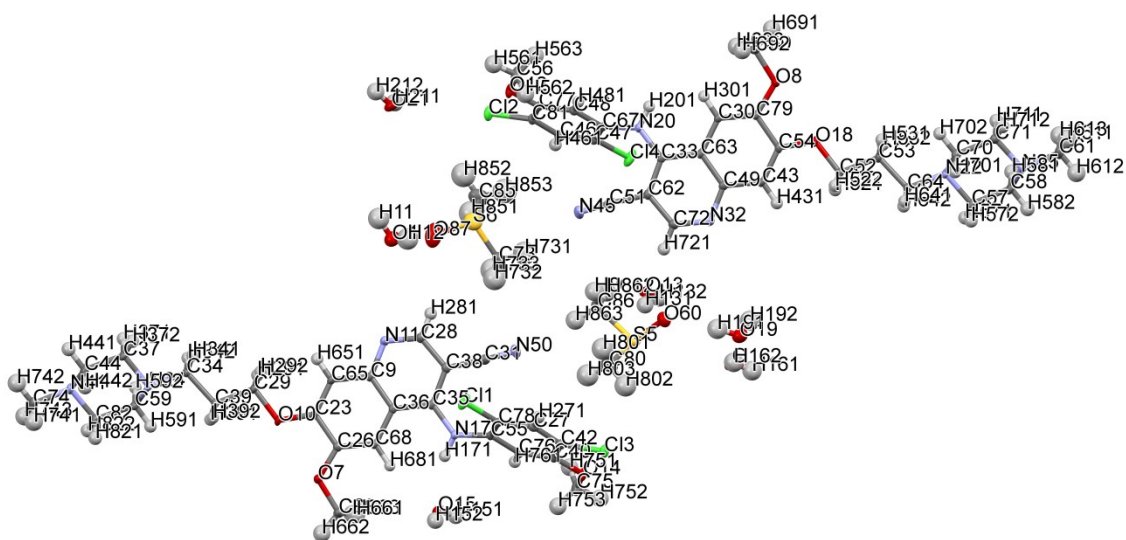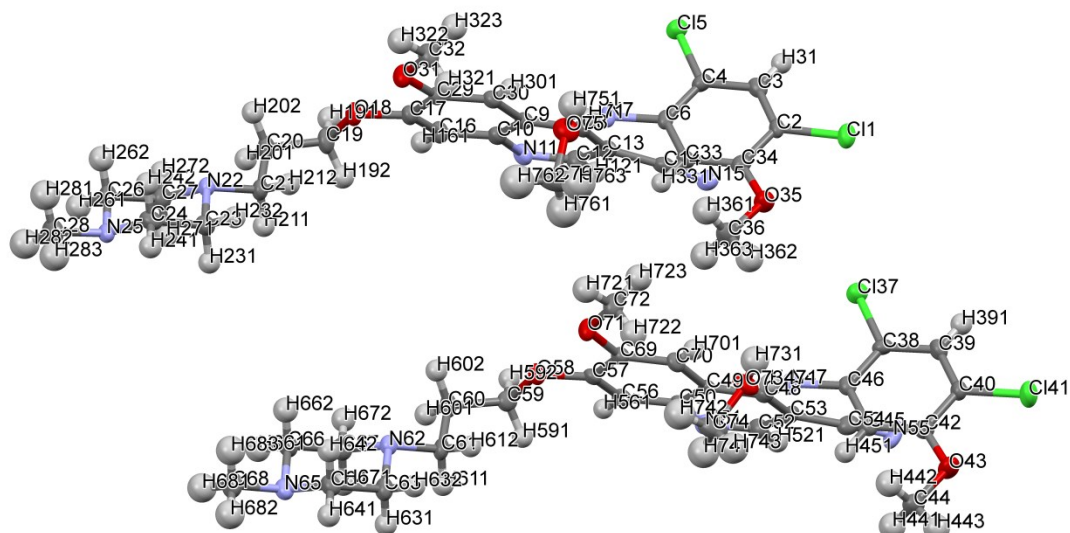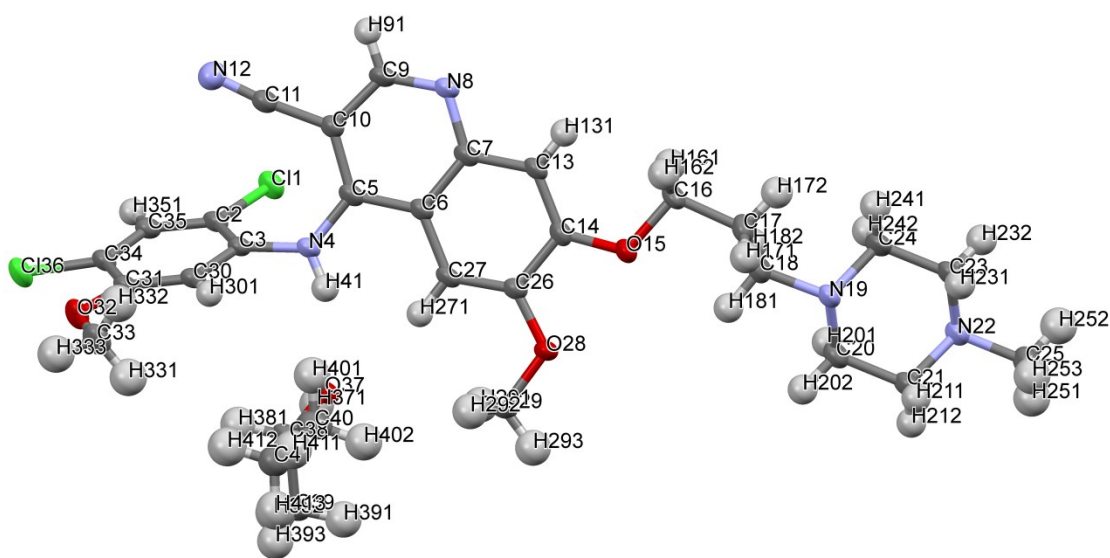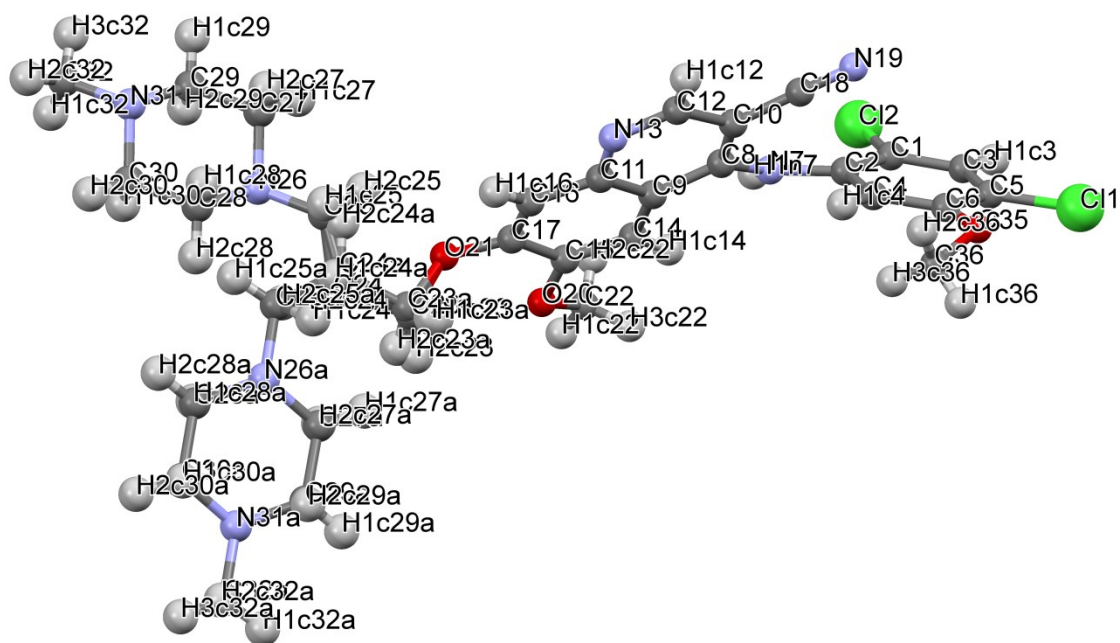**Figure S5** Molecular configuration and atom-numbering scheme for 2H$_2$O


Figure S6 Molecular configuration and atom-numbering scheme for 6H$_2$O
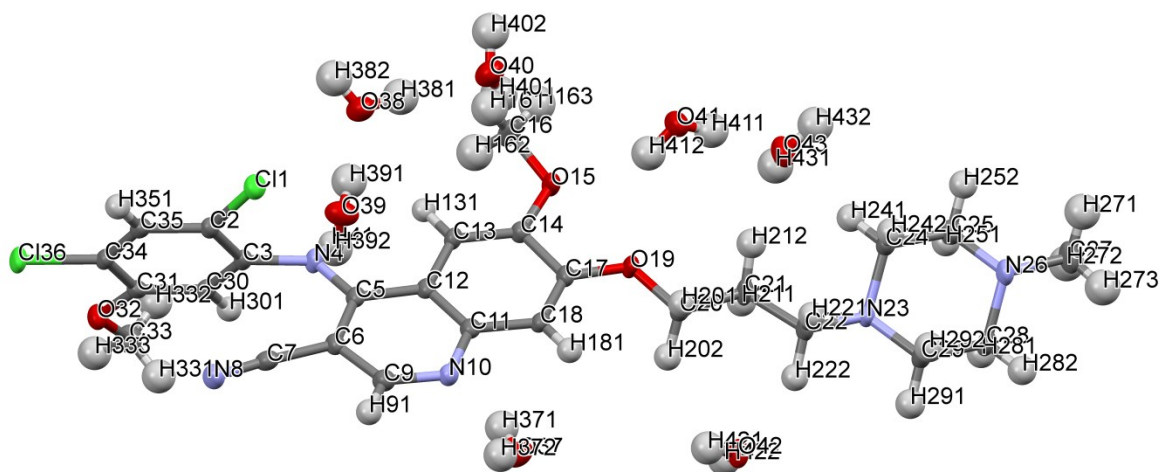
**Figure S7** Molecular configuration and atom-numbering scheme for 7H$_2$O
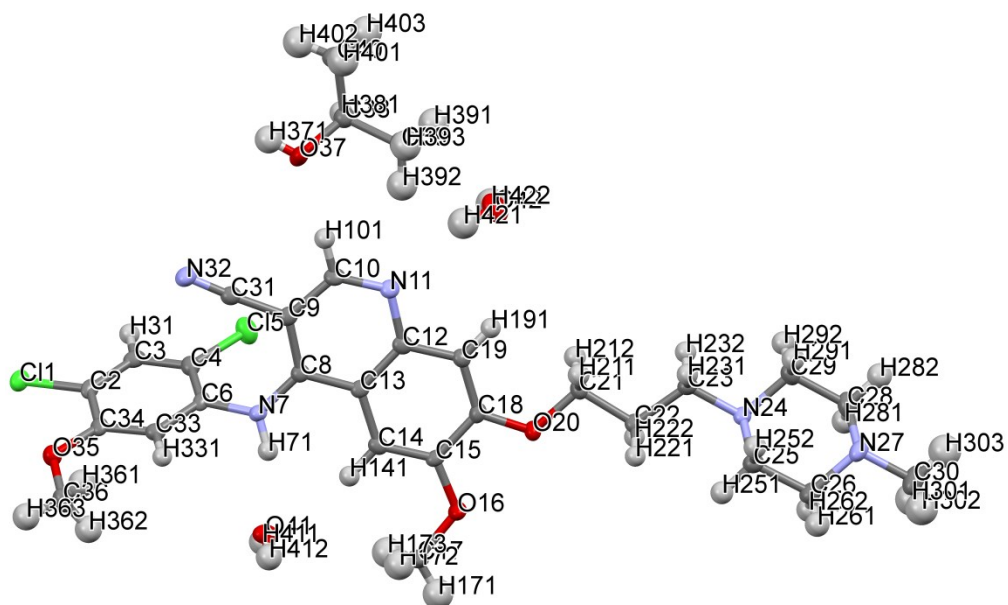
Figure S8 Molecular configuration and atom-numbering scheme for IPA-2H$_2$O
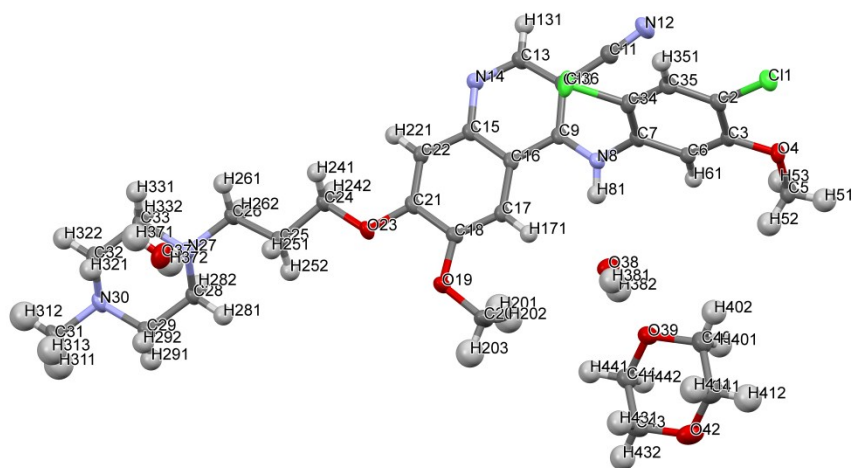
Figure S9 Molecular configuration and atom-numbering scheme for Diox-2H$_2$O

Figure S10 Molecular configuration and atom-numbering scheme for DMSO-3H$_2$O

Figure S11 Molecular configuration and atom-numbering scheme for MeOH

Figure S12 Molecular configuration and atom-numbering scheme for 2-BuOH

Figure S13 Molecular configuration and atom-numbering scheme for AH
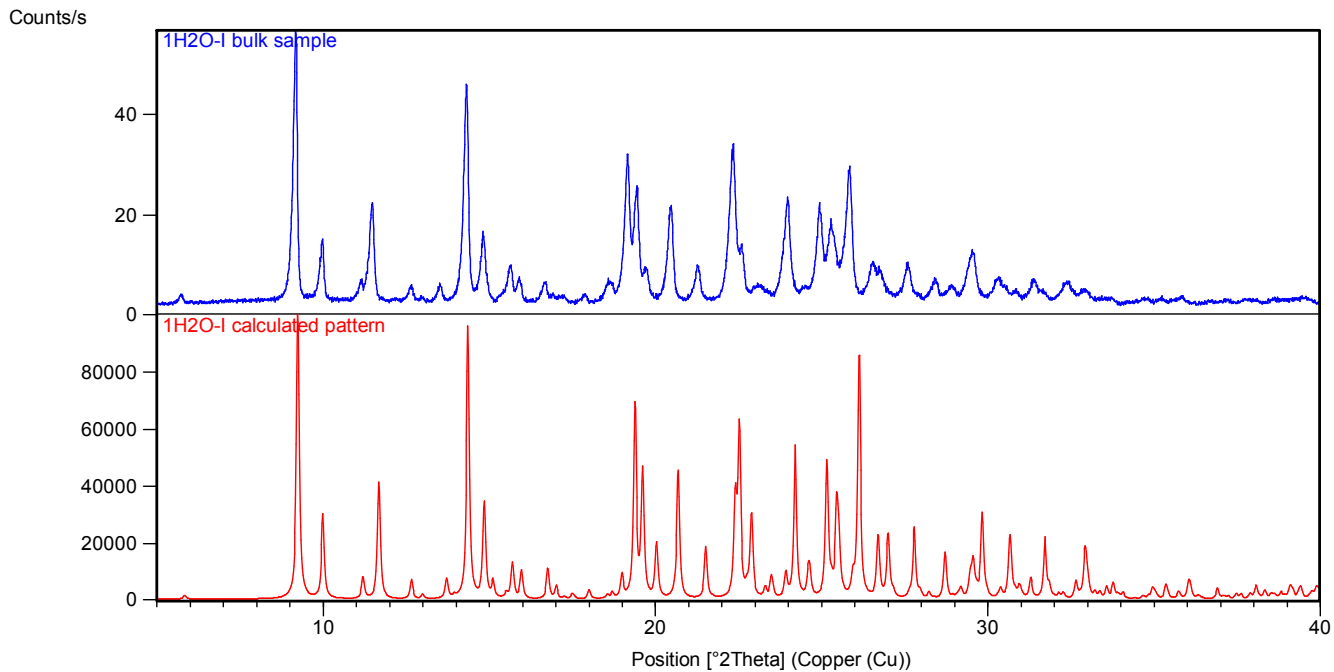
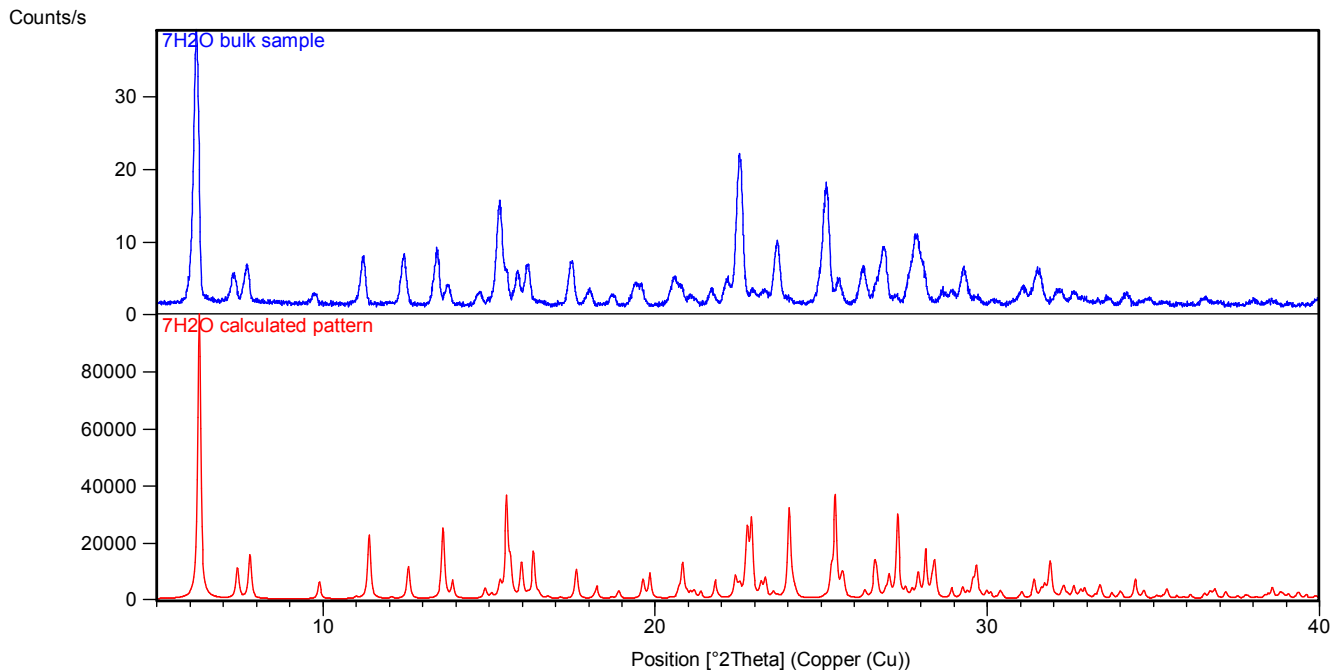**Figure S14** Measured, bulk and calculated pattern of 1H₂O-I
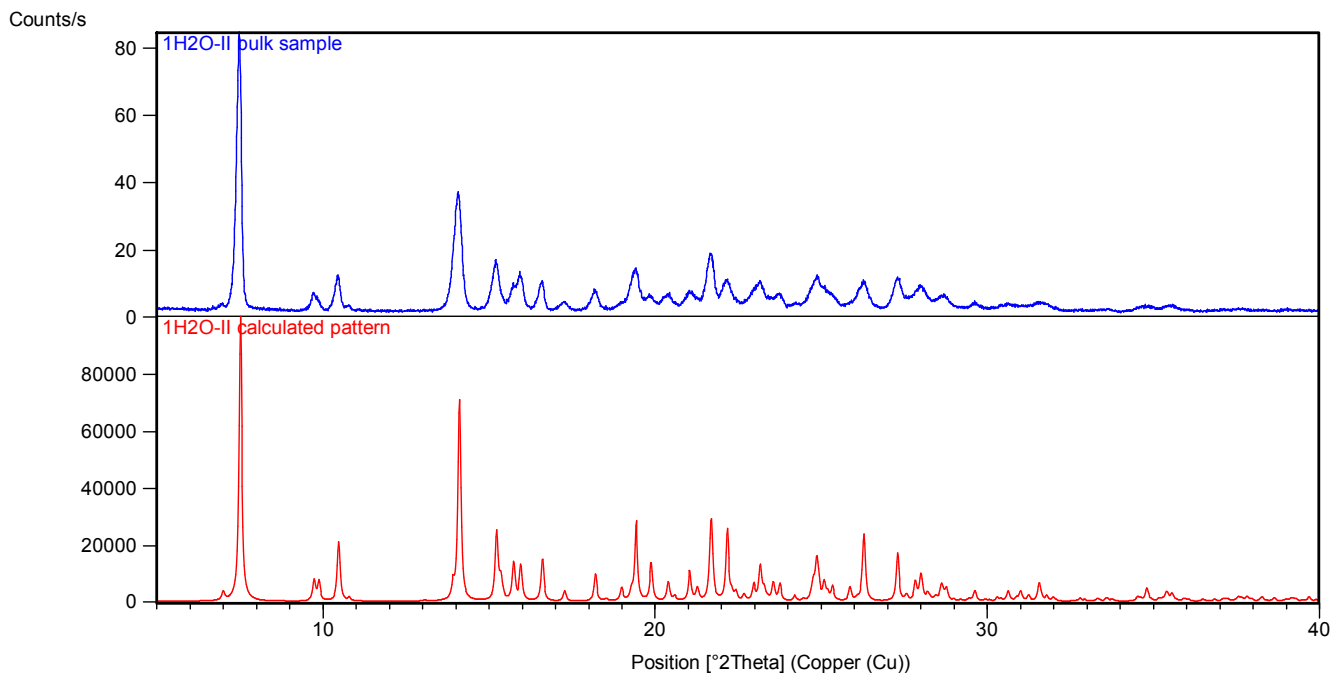
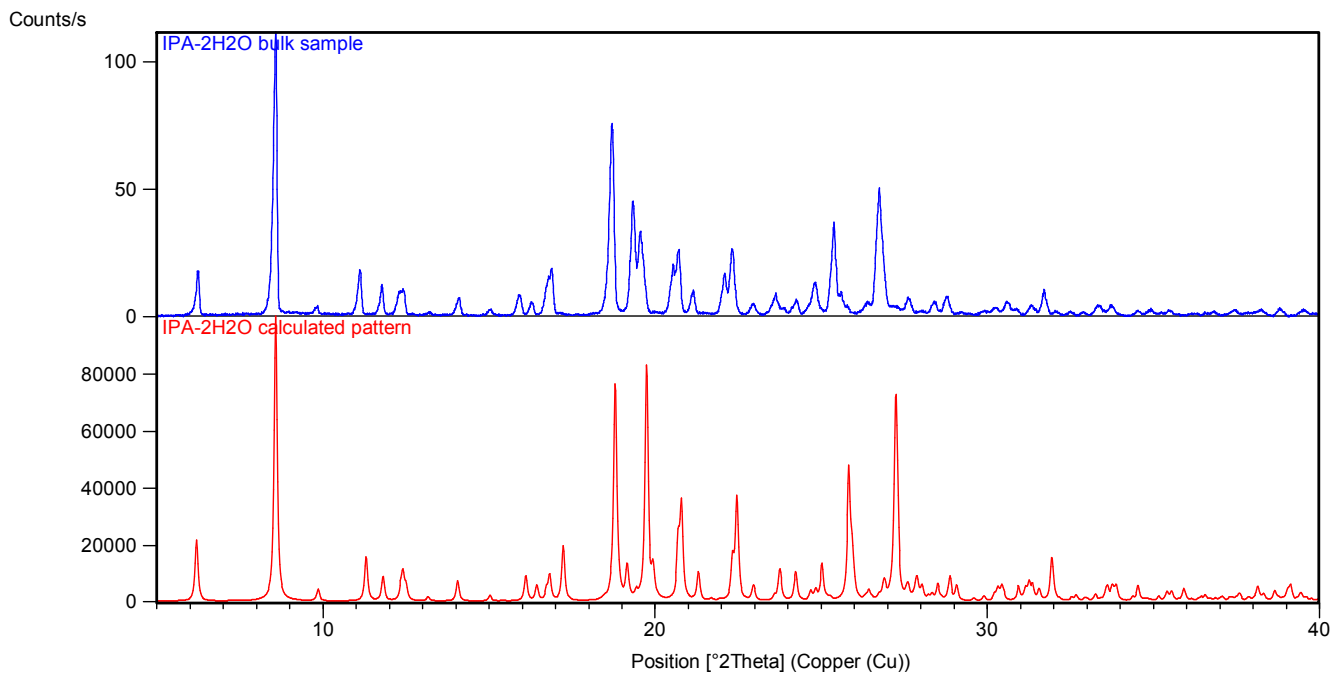**Figure S15** Measured, bulk and calculated pattern of 1H₂O-II
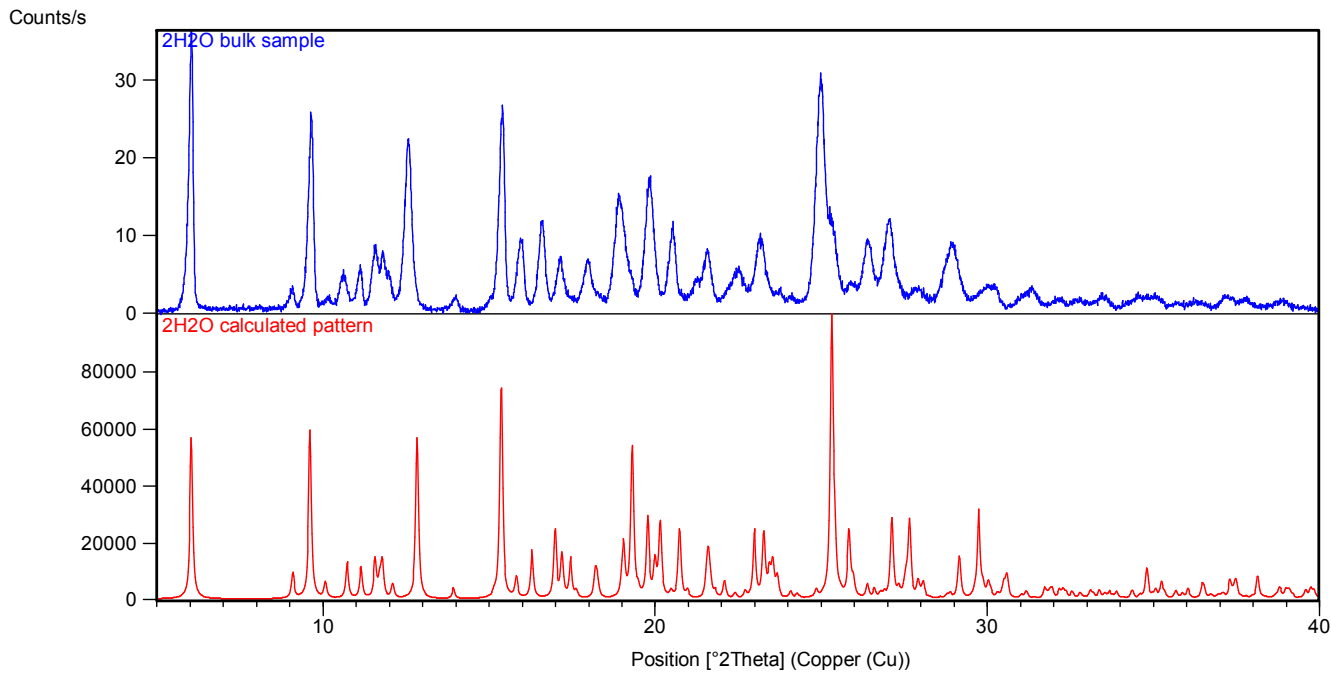
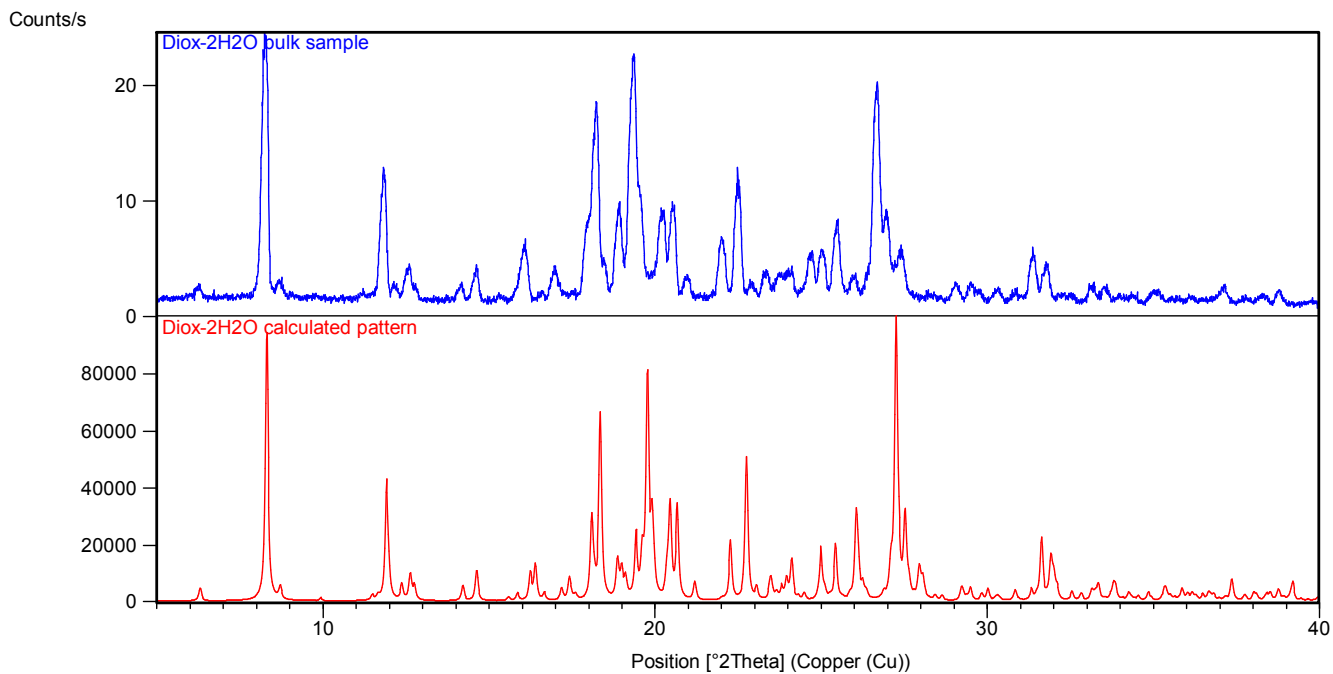**Figure S16** Measured, bulk and calculated pattern of $2H_2O$
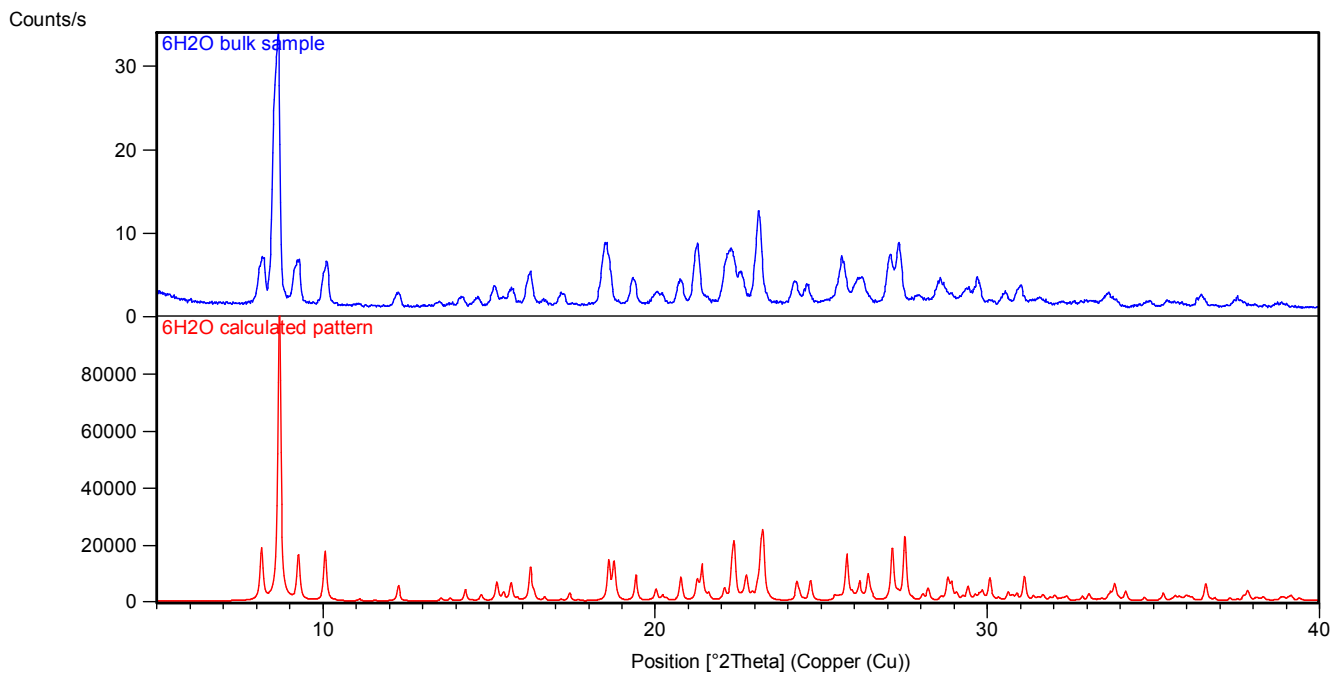
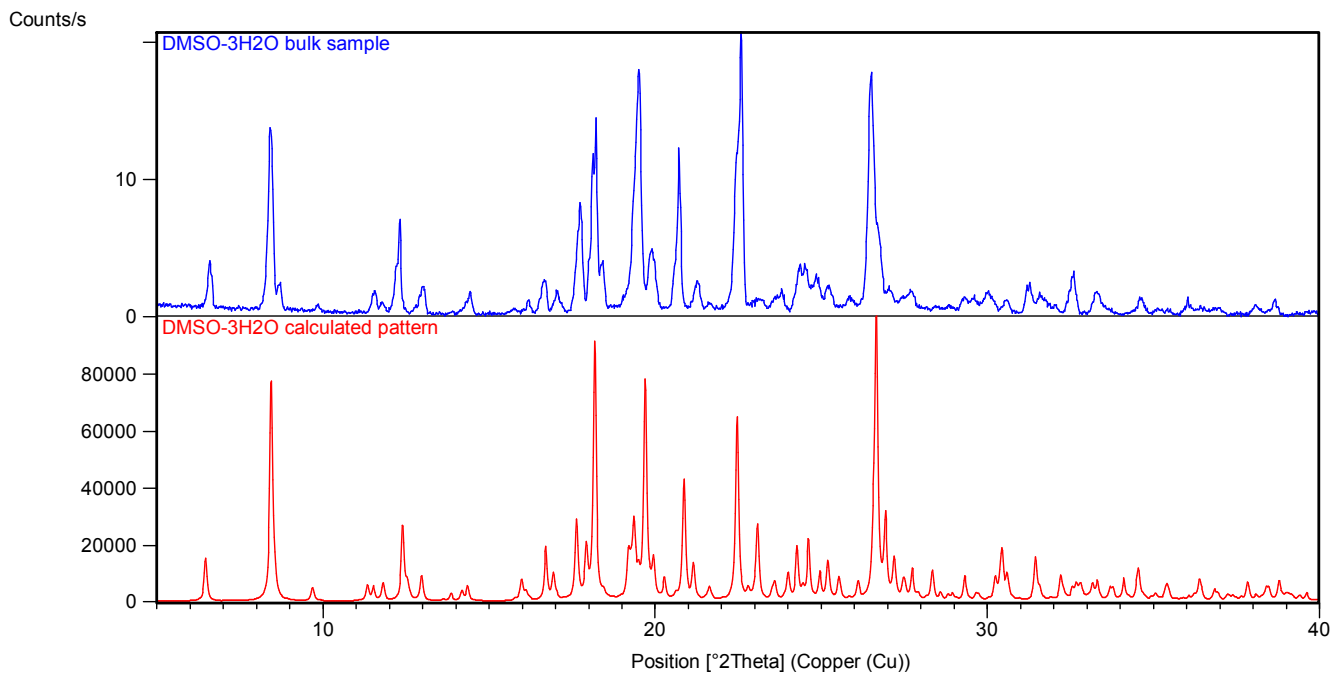**Figure S17** Measured, bulk and calculated pattern of $6H_2O$

Figure S18 Measured, bulk and calculated pattern of $7H_2O$
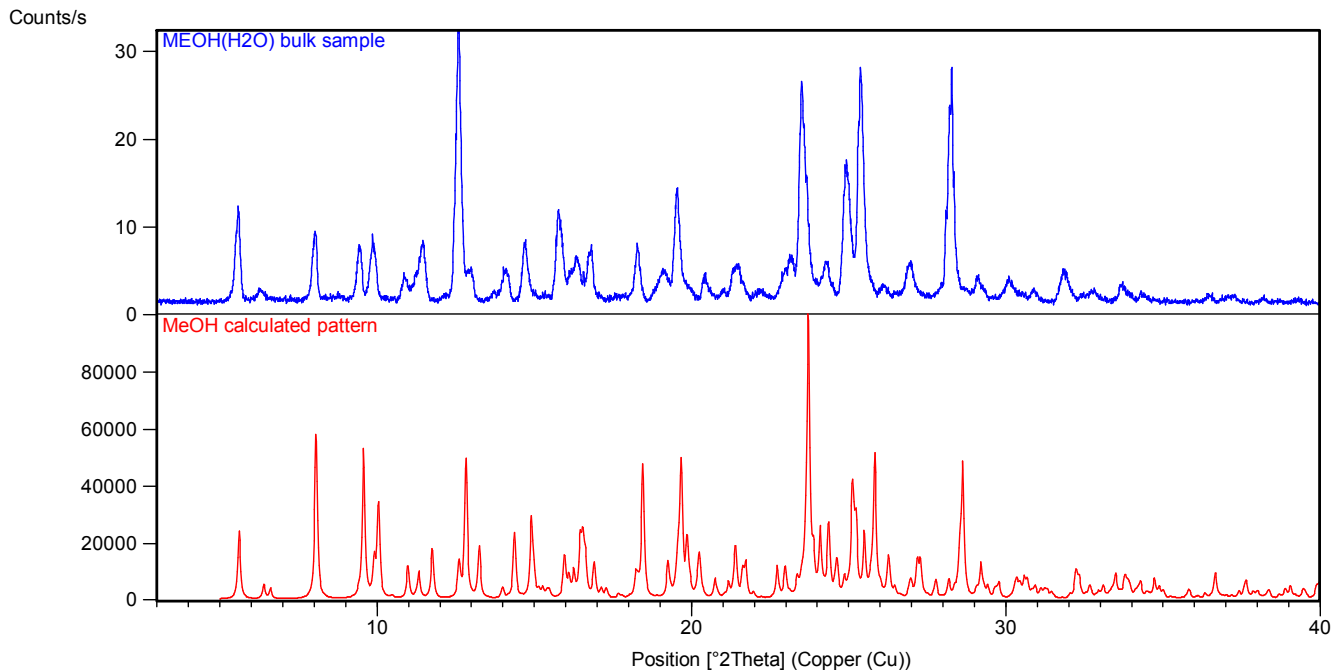

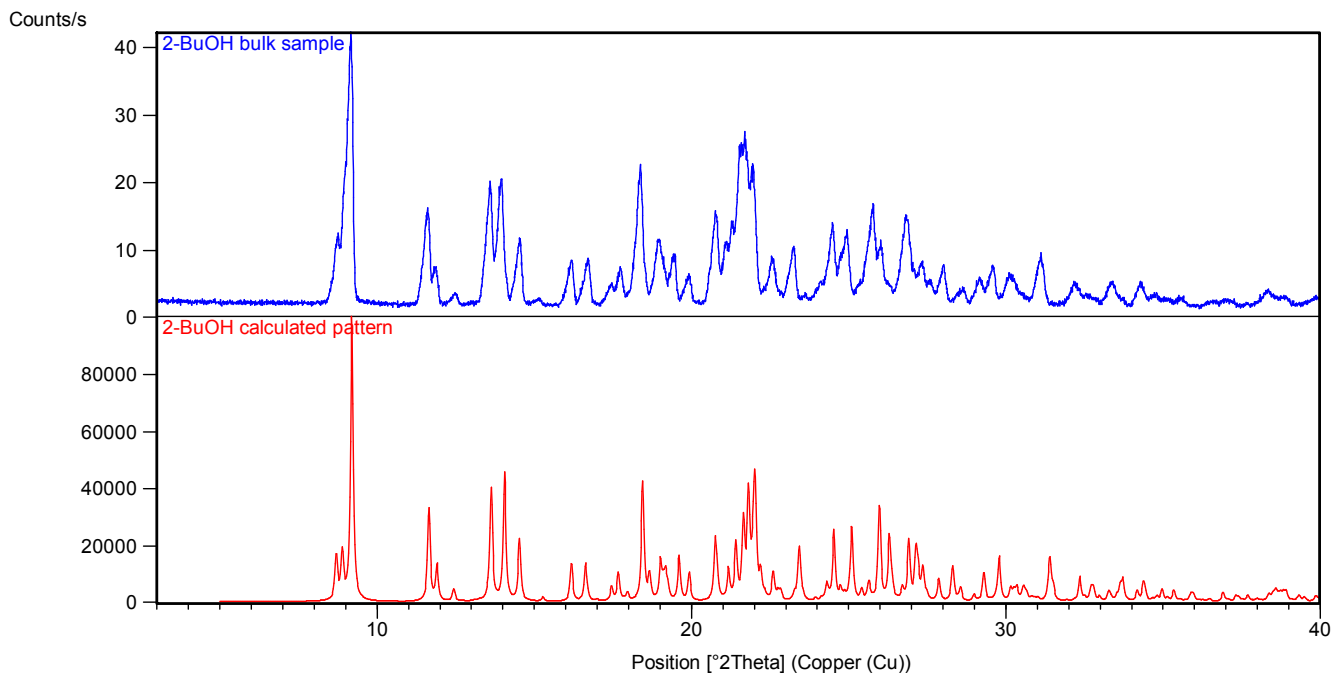**Figure S19** Measured, bulk and calculated pattern of IPA-$2H_2O$

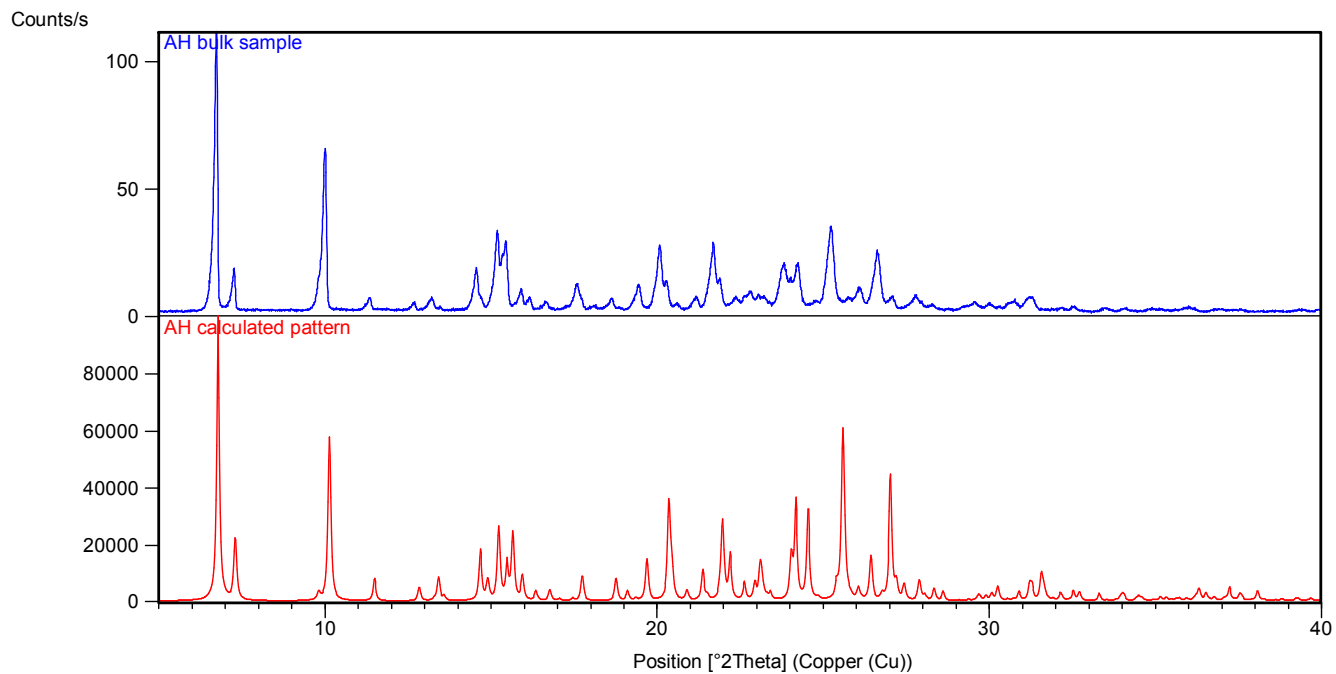**Figure S20** Measured, bulk and calculated pattern of Diox-2H$_2$O

Figure S21 Measured, bulk and calculated pattern of DMSO-3H$_2$O

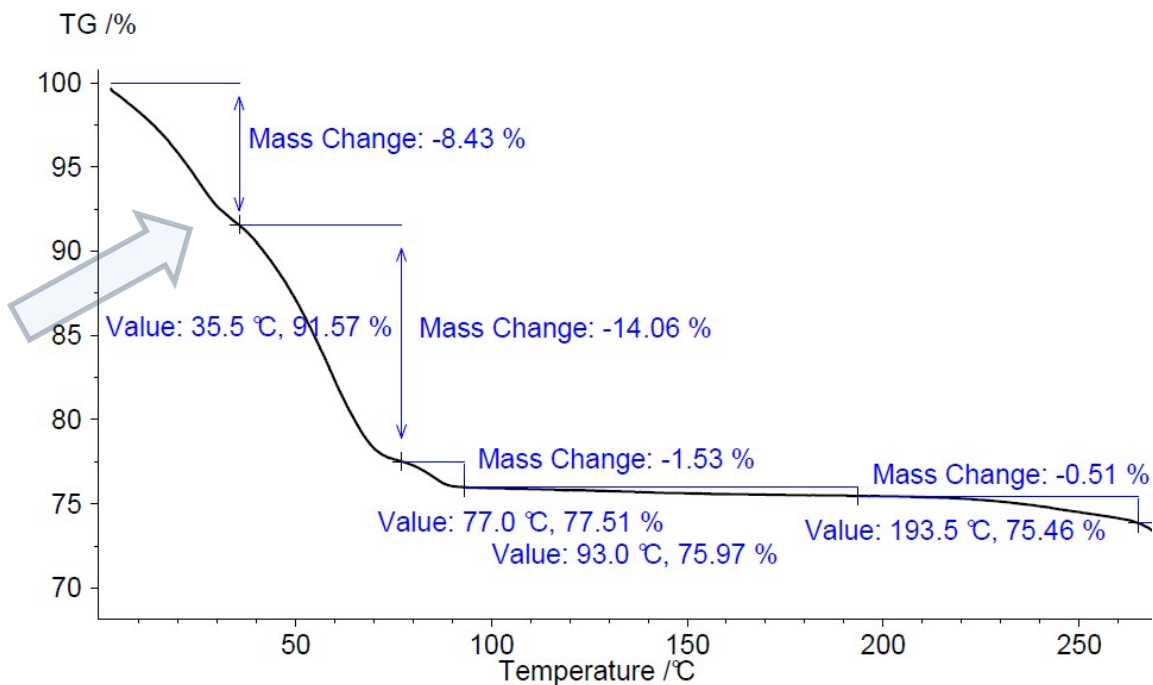**Figure S22** Measured, bulk pattern of MeOH(H$_2$O) and calculated pattern of MeOH

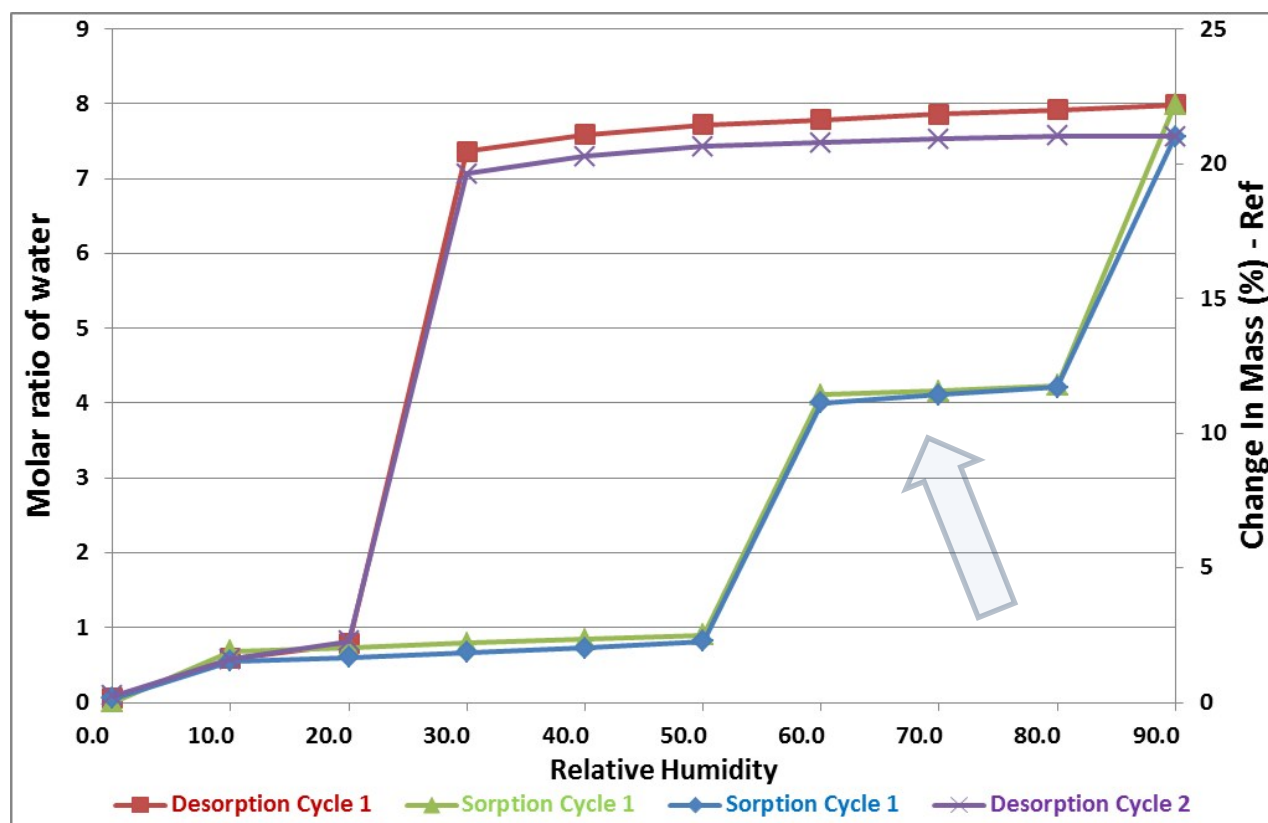**Figure S23** Measured, bulk and calculated pattern of 2-BuOH

Figure S24 Measured, bulk and calculated pattern of AH
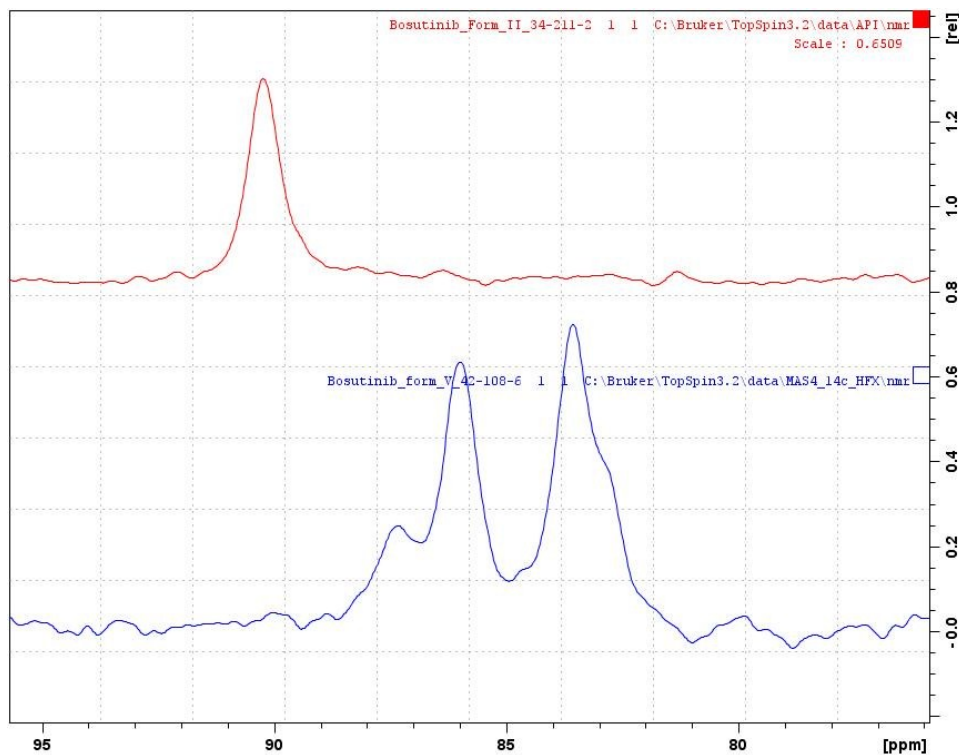
The evidence of a potential tetrahydrate

Figure S25 TG curve of $7H_2O$ showing an intermediate stage corresponding to 4 molar equivalents of water

**Figure S26** DVS isotherm of $7H_2O$ indicating the existence of a tetrahydrate

Disorder of AH


Figure S27 Segment of the ^{13}C ssNMR spectrum of **AH** and **1H$_2$O-II**

In the case of AH the signal of carbon bearing the CN group splits into four in the ratio of 1:2:1:2 in accordance with the occupancy of the two conformations (Figure S27).

The disorder is also visible in the Raman (Figure S28)and IR spectrum, as the peak of the nitrile group (around 2250 cm^{-1}) split into two, while every other phase exhibits a sharp, well-defined peak (except for the amorphous phase). This phenomenon clearly shows that two conformations are present in the structure, which possess different energetic state, therefore appear at different wavenumbers.
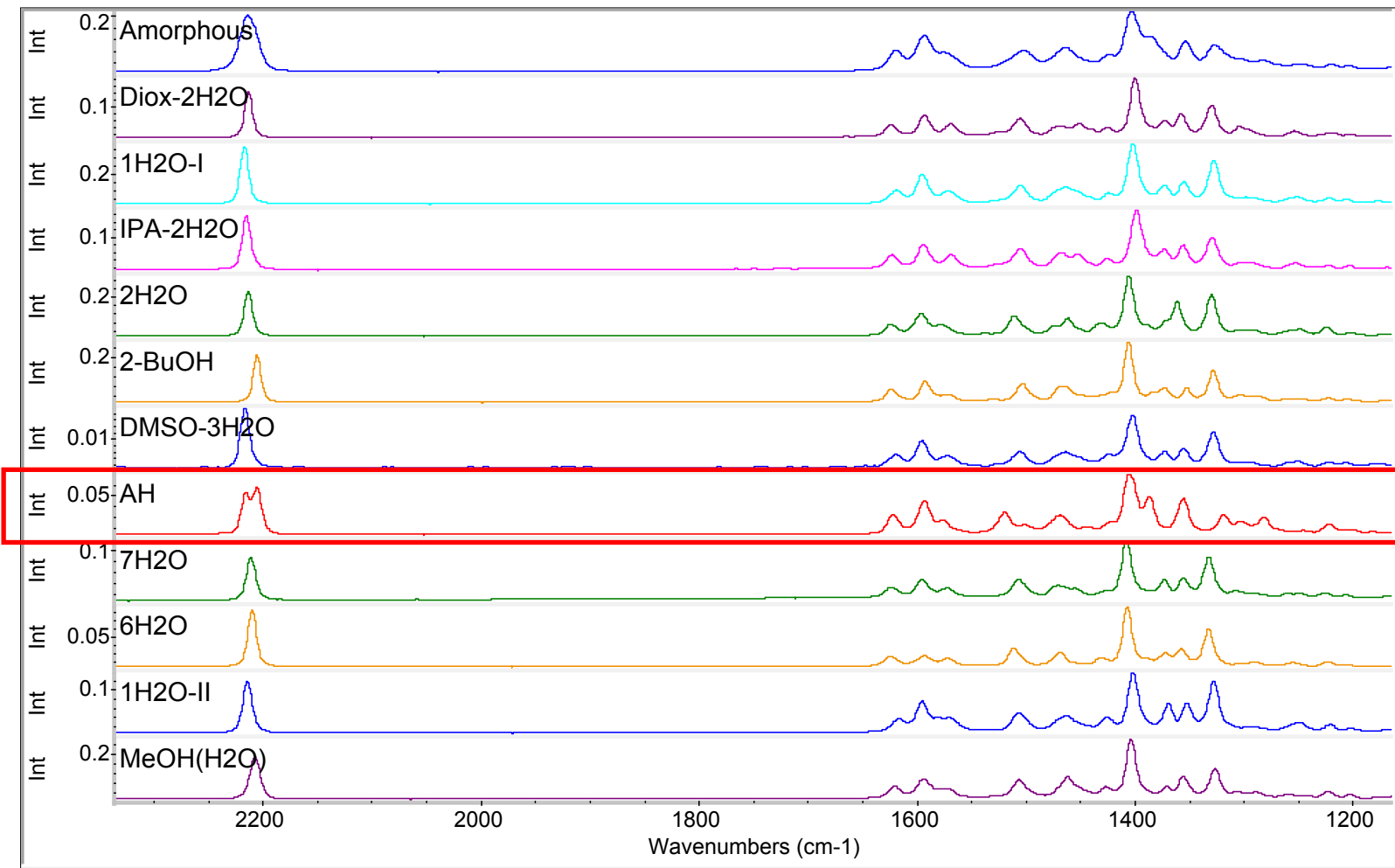
**Figure S28** Comparison of the Raman spectra of bosutinib forms
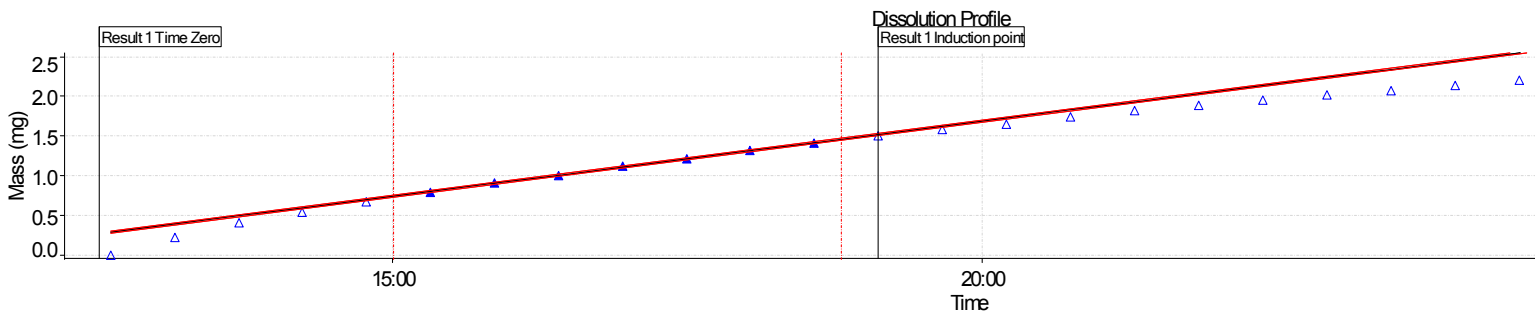
Figure S29. Intrinsic dissolution curve of AH

$7H_2O$ has the highest stoichiometry of all of the described solvates/hydrates of bosutinib. To compare the channels in the structures, we have selected two other forms with high solvent/water content and calculated their voids.

To display and analyze the solvent/water channels, first the solvent/water molecules were deleted from the cif file and then the void map was calculated using Mercury (contact surface, probe radius 0.8 Å and approx. grid spacing 0.7 Å). As can be seen in the figure below, in all three bosutinib solvates/hydrates channels are present and are visually comparable in size. However, the calculated value of the void space indicates, that the channels are the largest in the $7H_2O$ structure.

The calculated void space in $7H_2O$ is 25.7%, in DMSO-$3H_2O$ 24.0% and in $6H_2O$ 22.4%.
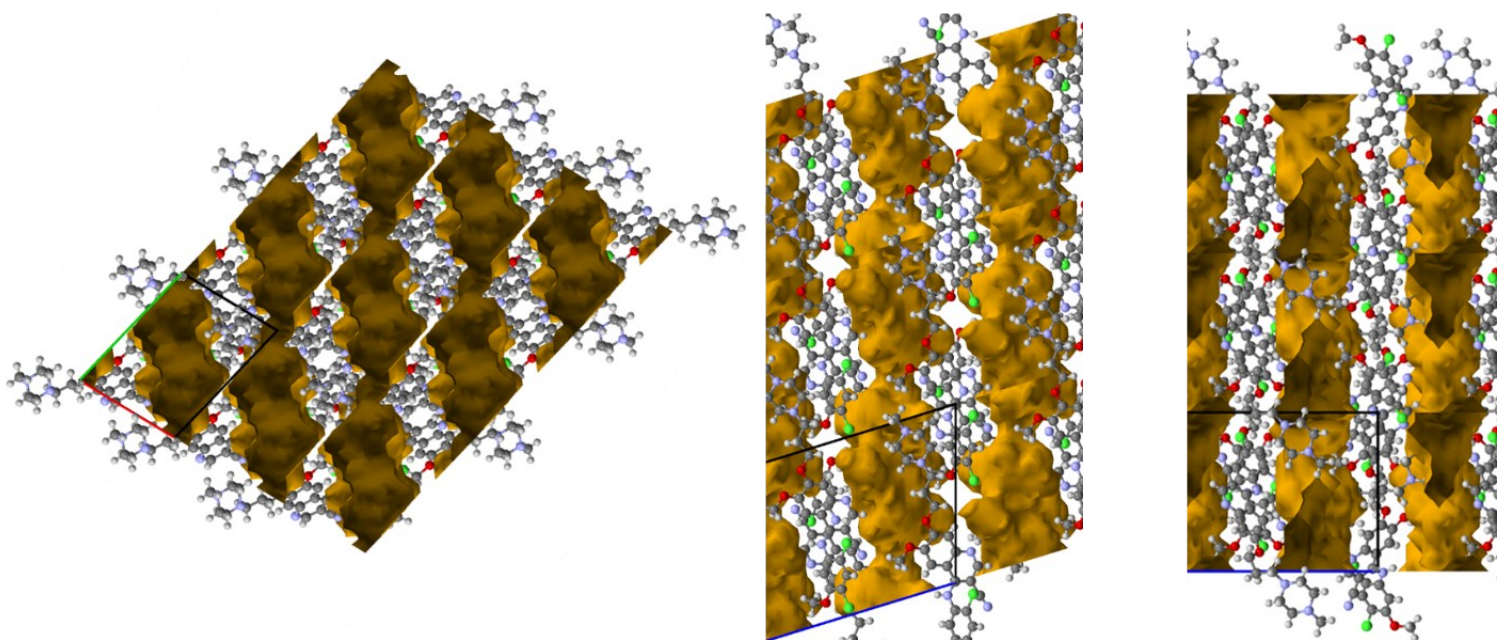
Figure S30. Void space in the structure of $7H_2O$ (left), DMSO-$3H_2O$ (middle) and $6H_2O$ (right)